Available online at www.CivileJournal.org

Civil Engineering Journal

(E-ISSN: 2476-3055; ISSN: 2676-6957)

Vol. 9, No. 08, August, 2023

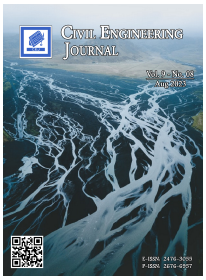

Effect of Curing Temperature on Mechanical Properties of Sanitary Ware Porcelain based Geopolymer Mortar

Woratid Wongpattanawut [1], Borvorn Israngkura Na Ayudhya [1*]

[1] *Department of Civil Engineering, Rajamangala University of Technology Thanyaburi, Pathum Thani, 12110, Thailand.*

Received 31 March 2023; Revised 10 July 2023; Accepted 19 July 2023; Published 01 August 2023

Abstract

The objective of this study was to investigate the effect of curing temperature on the mechanical properties of sanitary ware porcelain powder-based geopolymer paste and mortar under various curing temperatures. The setting time, porosity, water absorption, and compressive strength of specimens mixed with alkaline concentrations of 8M, 10M, 12M, and 14M were compared. All mortar cube (50×50×50 mm) specimens were placed into drying ovens for 24 hours at 60°C, 75°C, 90°C, and 105°C, respectively. The specimens were then air-cured for 1, 3, 7, 14, and 28 days. The results showed that the elevated curing temperature accelerated the polymerization process of the porcelain geopolymerization reaction. The setting time varied between 89 mins and 380 mins. It showed variability depending on alkaline concentration and initial curing temperature. The setting time of pastes decreased when alkaline concentrations increased. An increasing temperature in the drying oven decreased the initial and final setting times. Similar to this, the rate of water absorption and permeability of porcelain-based geopolymer mortar specimens decreased with drying oven temperatures and increments in alkaline concentration. The lowest water absorption and porosity of the specimen were 2.1% and 15.7%, respectively. The compressive strength increased as drying oven temperatures and alkaline concentrations increased. The highest 28 day compressive strength was found in 14M specimens with 105°C curing temperatures. The ultimate compressive strength was 64.45 N/mm^2. Scanning electron microscopy (SEM) and X-ray diffraction (XRD) were investigated to study the microstructural properties of the geopolymers.

Keywords: Geopolymer; Setting Time; Porosity; Porcelain; Mortar.

1. Introduction

During the period of 2010-2020, the global demand for sanitary ware has grown up by 53%, from 2.16 to 3.3 million tons. Asia holds the largest consolidated global sanitary ware exporter position with 62.6% of the total global export share. While Thailand shares 3% (87,129 tons) of global export sanitary ware [1]. In domestic consumption, sanitary ware shares 44.8% of total production (1.83 million pieces) [2]. Sanitary ware is categorized as a white ceramic product that consists of kaolin having low amounts of iron oxide. However, it has been estimated that the good performance of the production process causes defective products around 5–12% of total daily production. There are three main waste types from porcelain sanitary ware production: porcelain mud wastes (PMW), crushed porcelain wastes (CPW), and porcelain dust wastes (PDW). The use of waste porcelain in experiments is primarily focused on its environmental impact. The geopolymerization technique is a promising and environmentally alternative decision that can alleviate waste pollution problems. By replacing either partially or totally the amount of waste material, it helps to reduce CO_2 emissions and utilize waste material.

* Corresponding author: borvorn_i@rmutt.ac.th

http://dx.doi.org/10.28991/CEJ-2023-09-08-01

Currently, alkali-activated materials (AAM) can be categorized into two levels of calcium content. First, a binder with high calcium oxide content (fly ash class C, blast furnace slag, and silica fume). Second, a binder with low calcium oxide content (fly ash class F, rice husk, and metakaolin). Ceramics and porcelain have similar in raw material compositions. Both material compositions have low in calcium oxide. The differences between ceramic and porcelain are the rate of material absorbs water, density, and durability. Most porcelain tiles/sanitary ware absorb less than 0.5% of water, while ceramic has a higher ability to absorb water. Density of material: porcelain has a high density, which leads to less in porosity when it is compared with ceramics. As far as durability is concerned, porcelain is denser than ceramic and therefore less porous. Porcelain is harder, more durable, and lesser absorb water. Table 1 shows the results of other researchers' studies on porcelain and ceramic-based geopolymers. For sanitary ware porcelain, the major raw materials used are kaolin, clay, feldspar, quartz, and ground-fired waste. These raw materials are mainly composed of SiO_2 and Al_2O_3. The feldspar is acting like a fluxing agent for densification, promoting the formation of a liquid phase. This phase eventually becomes denser with low porosity and high amorphous content [3]. Thus, it gives a potential alternative choice as a substitute cementitious material [4]. The strength of geopolymer depends on various factors, including curing temperature and curing duration [5, 6].

However, the selection of the alkali activator, alkali concentration, and chemical composition cannot be overviewed. A comprehensive review of the low-calcium geopolymer binders shows slow reactivity at ambient temperature. Reasonable heat (above 60°C) must be applied to enhance the geopolymerization process. In addition, both curing temperature and curing time affect the durability of geopolymer specimens [7]. The reduction in water content also affects the concentration of alkali activator, which substantially assists the chemical reaction. Hence, an increase in the concentration of sodium hydroxide results in durability. The workability and durability of low-calcium binder-based geopolymer paste are influenced by the properties of the constituent material [8]. The properties of the alkaline silicate solution had a great impact on the characteristics of viscosity and setting of the geopolymer paste [9]. The slump of fresh geopolymer concrete increases as the water content of the mixtures increases. The compressive strength of geopolymer concrete decreases as the molar ratio of H_2O to Na_2O increases. For this reason, reviews have drawn attention to the study of the mechanical properties of kaolin geopolymer (low-calcium) porcelain mortar-based alkaline activators. Although ceramic and porcelain can be made with low calcination temperatures, the interaction of various parameters on workability and mechanical properties of geopolymer paste is still complex. In addition, utilizing sanitary ware porcelain waste from the porcelain sanitary ware industry is encouraged. Therefore, several parameters of low-calcium porcelain-based geopolymer paste and mortar are subjected to testing to establish the effect of curing temperature and curing time on setting time, workability, and compressive strength of porcelain-based geopolymer mortar.

Table 1. Cases of geopolymer –based and curing temperature

Case	Strength (N/mm^2)	Curing Temp (°C)	Curing Period	Reference
Porcelain	30.0 paste	65	7	Luhar et al. (2021) [10]
Ceramic	24.3 paste	90	7	Shoaei et al. (2019) [11]
Ceramic	20.9 paste	60	7	Shoaei et al. (2019) [11]
Porcelain	36.0 paste	65	7	Reig et al. (2013) [12]
Metakaolin	98.0 concrete	60	7	Mo et al. (2014) [13]
Furnace Slag	38.0 paste	60	3	Naral et al. (2014) [14]

2. Materials and Experiment Methods

The temperature helped to increase the degree of kinetic reaction in which silica and alumina dissolved. As a consequence, the bond strength of geopolymers increased. The optimum temperature for maximizing strength could be varied. Depending on the type of binder material used, it ranged from 60°C to 90°C [8–10]. It was further found that curing temperatures between 40-80°C for 4 to 48 hours were vital aspects for the synthesis of geopolymer materials [15, 16]. The length of curing time affected the moisture content level of geopolymer specimens, which caused significant shrinkage, the formation of cavities and cracks, and reactions in the geopolymer. The longer period of curing time led to water loss, which caused carbonation and delayed the activation of precursors. The appropriate thermal curing at mid-range temperature was around 60°C–70°C up to 7 days [17–19]. In addition, the temperature of the initial geopolymer paste affected the formation of minerals and the physical and mechanical properties of metakaolin-based geopolymer pastes. A higher initial paste temperature accelerated the formation of geopolymer structures [20].

For terracotta tile, a curing temperature of 65°C for 24 hours gave the optimum yield [21]. For high-strength geopolymer concrete, an increase in curing time and additive material (superplasticizer) dose were required [22]. In order to increase the further compressive strength of geopolymer material, a larger particle size of reinforcement material (> 0.6 mm) was needed with a curing temperature of 50°C [23]. For the ultra-high-strength concrete, sanitary ceramic wastes were used as fine and coarse aggregate. It was found that sanitary ceramic material helped to increase compressive and tensile strength by about 24.74% and 34.25%, respectively [24]. Regarding external temperature, the

temperature of the thermal load applied to the specimen affects the flexural and compressive strengths of porcelain-based geopolymer waste (an electrical insulator). The ultimate strength of compressive force (95 N/mm^2) was found when the temperature of the thermal load was at 1,200°C [25]. The literature on porcelain-based geopolymers for sanitary ware was limited. Most researchers studied other low-calcium materials, such as fly ash class F and metakaolin. It might be due to the scrutiny process of hammering, grinding, and sieving. The technical data on the effect of curing temperature and alkaline solution on such paste and concrete was further needed. This paper focused on the suitability of the curing temperature of porcelain-based geopolymer powder in terms of mechanical properties. The authors selected the three most crucial factors in this study to comprehensively understand the effects of curing temperature, curing period, and modulus ratio on porcelain-based geopolymer pastes and mortars.

2.1. Materials

The porcelain waste was collected from a sanitary ware manufacturer in Saraburi province. The raw material was largely composed of kaolin, clay, feldspar, flint, calcium carbonate, dolomite, and sodium silicate. The sanitary ware porcelain waste was initially reduced to 10 mm in size by a crushing machine. The particles were further reduced by grinding and steel ball mill machine (passing sieve No.200 (75mm) (Figure 1), which was then kept in a sealed container.

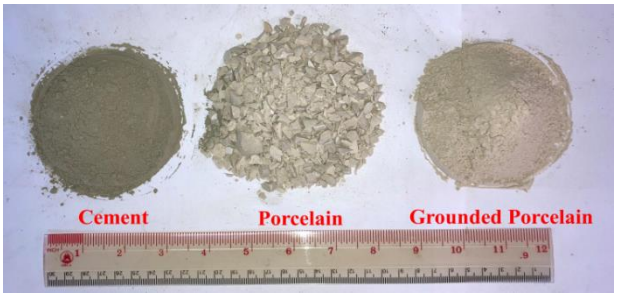

Figure 1. Raw materials used for preparing specimens

The sodium hydroxide used in this study was in flake shape (NaOH, 99.9%). It was an alkali source to produce the alkali-activated binder (AAB). A sodium silicate solution (Na_2SiO_3) with 11.67% Na_2O, 28.66% SiO_2, and 59.67% H_2O was used as a liquid activator. A fine aggregate was a land-based sand with particle sizes less than 0.475 mm. The specific gravity in SSD condition and water absorption of the fine aggregate were 2.67 and 0.25%, respectively. A scanning electron microscopy (JSM-IT500HR model) was used to analyze the morphology of cement and porcelain powder. Micrographs with high magnification (500X and 10,000X) of the surfaces of cement and porcelain powder are shown in Figure 2. It could be seen from 500X magnification that OPC contained smaller particles than porcelain. In 10,000X magnification, it appeared that the porcelain element had a more flat and shaped edge. Therefore, the morphology of porcelain is irregular, and the particles vary in shape and size. The particles of porcelain used were angular since the material was crushed by a grinding machine. In order to reduce the internal friction of the mixture and improve its workability, superplasticizer was used to increase its workability [26].

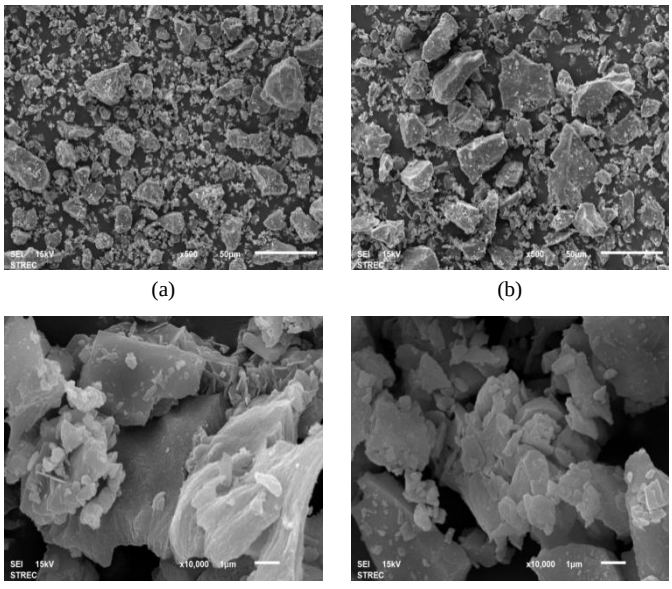

(a) (b)

(c) (d)

Figure 2. SEM particle images of (a) OPC at 500X (b) Porcelain at 500X (c) OPC at 10,000X

Figure 3 shows the comparative particle size distribution of OPC and porcelain powder, which was determined by a laser particle size analyzer (Mastersizer 3000 model). The porcelain particles were larger than those of OPC. The average particle size, d_{90}, of porcelain and OPC was 51.43 mm and 32.70 mm, respectively. Both specimens presented an optimum pore size of 31.1 mm and 16.4 mm, respectively. The OPC particles were largely in micro-porosity material, whereas mesoporosity was mostly in the geopolymer-based porcelain. The porcelain consisted mainly of SiO_2 (54.90%) and Al_2O_3 (17.50%), while OPC consisted mainly of CaO (62.70%) and SiO_2 (17.80%). These major oxides play roles in alkaline activation and hydration, respectively [9]. For metal oxides having composition, porcelain has 4.48% ($CaO+Fe_2O_3$), whereas OPC has 65.58% ($CaO+Fe_2O_3$). These summations of oxide composition had an impact on compressive strength [14]. The greater values of summation of metal oxide composition, the higher the compressive strength that could be obtained. Additionally, the analysis of mineralogical compounds of OPC and porcelain powder was also further investigated by X-ray diffraction (XRD; Bruker D8 Discover model), which provided the chemical composition (Table 2).

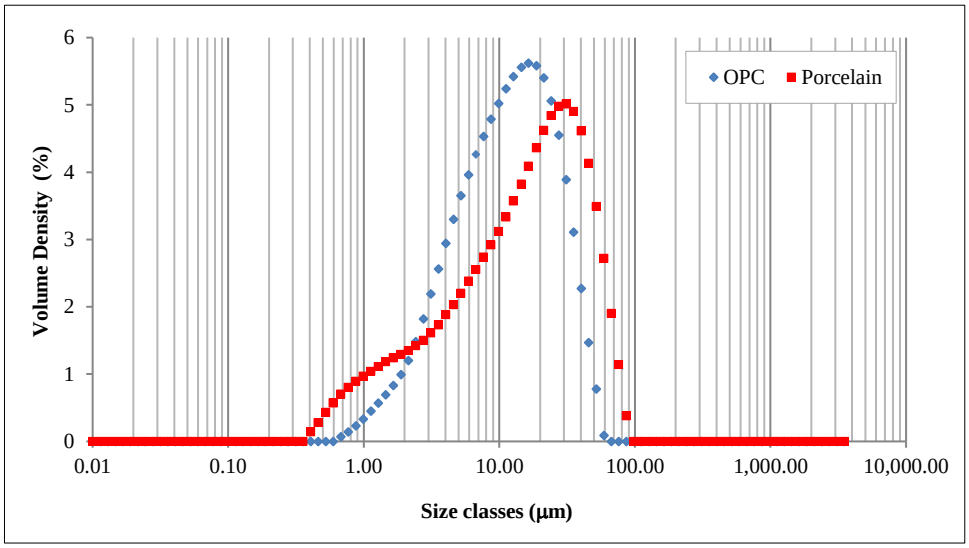

Figure 3. Particle size distribution of OPC and Porcelain

Table 2. Composition of OPC and Porcelain material

Oxide	OPC	Porcelain
CaO	62.70	2.85
SiO_2	17.82	54.90
Al_2O_3	3.82	17.50
SO_3	2.90	0.01
Fe_2O_3	2.88	1.63
MgO	1.84	0.55
K_2O	0.48	2.99
TiO_2	0.30	0.30
Na_2O	0.28	1.09
Cl	0.19	0.05
P_2O_5	0.10	0.06
MnO	0.05	0.04
SrO	0.03	0.01
ZnO	0.03	0.47
CuO	0.02	<0.01
ZrO_2	0.01	0.67
Rb_2O	-	0.03
NiO	-	0.01

Figure 4 shows crystalline phases obtained by XRD. It was found from porcelain powder specimens that the predominance of SiO_2 (Quartz, Q) and $Al_6Si_2O_{13}$ (Mullite, M) and $Fe_2(SiO_4)$ (Fe-Ringwoodite, Fe), which consisted of

silicon and oxygen, were mainly found. However, mullite was formed during the heat-sintering process in porcelain production [27]. It was a common phase in electrical insulators in which quartz and mullite were found [28, 29]. While XRD patterns for calcined kaolin-based geopolymer paste had higher crystalline peaks. The crystalline peaks of porcelain were lower than those of calcined kaolin by approximately 1,700 counts [30, 31]. From the mineralogical composition analysis result, porcelain could develop further reactions as a secondary aluminosilicate source in the alkali-activation process. While cement found calcium silicate (Ca_3SiO_5), calcium silicate oxide [Ca_3 (SiO_4)O], lizardite ($(Mg,Fe,Ca_3)(Si,Al_2)O_5(OH)_4$), and Magnesia (MgO). In this study, the specimens were prepared by using porcelain ground powder as a precursor, a solution of sodium hydroxide and sodium silicate were used as an alkaline activator, mixed with sand as a fine aggregate. The alkaline activator solution (AAS) was prepared by using sodium hydroxide flake with sodium silicate solution. The ratio of AAS/binder is 0.7.

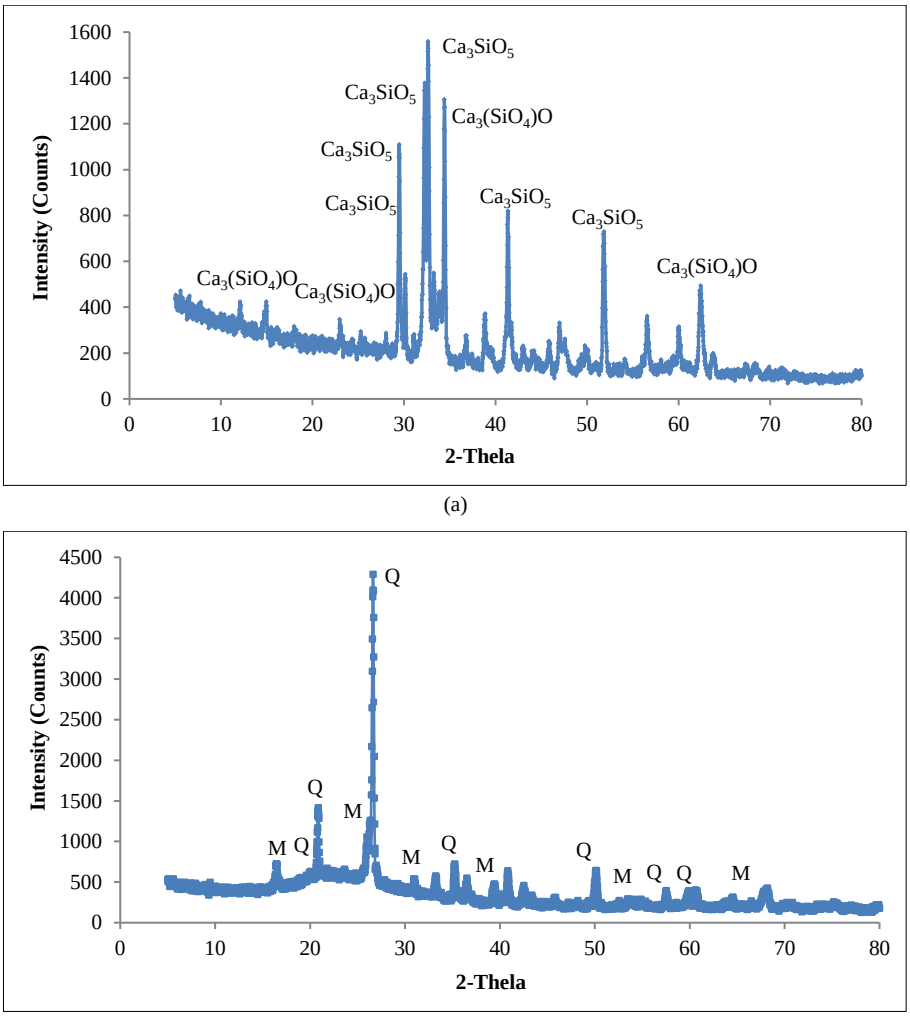

(a)

(b)

Figure 4. X-Ray diffraction analysis of (a) OPC and (b) porcelain

The concentrations of NaOH were 8M, 10M, 12M, and 14M. The AAS was fixed at 550 kg/m^3. The preparation of specimens was divided into two parts. First, preparation of geopolymer paste. Geopolymer pastes were subjected to initial and final setting time tests and flowability tests. Ground porcelain was stirred in the mixing pan for 5 minutes, then the alkaline solution was gradually introduced to the mixer. It was continuously mixed for 5 minutes. Homogenous paste was ready for setting time and the mini-slump test. The flowability of the paste was evaluated by measuring the diameter of the paste spread. Second, preparation of geopolymer mortar. Dry porcelain powder was mixed in a mixer for 3 minutes. The alkaline activator solution was added to the mixer and blended for 5 minutes. Fine aggregate was added to the mix, which continued for another 5 minutes. As a consequence, geopolymer mortar was poured into mortar molds for absorption, porosity, and compressive strength tests as described in the experiment methods. Immediately after each placing end, all filled molds were cured in the oven at various temperatures for 24 hours. After the oven curing period ended, all specimens were allowed to cool down at room temperature for 2 hours before being demolded and wrapped with polypropylene film. These demolded specimens were kept at room temperature condition until testing date. The temperature and relative humidity of each day were recorded.

2.2. Experimental Methods

All specimens were both oven-dried and air-cured. The curing of the specimens was divided into two steps. First, 24 hours oven-dried. All specimen pastes and mortars were subjected to four curing temperatures (60°C, 75°C, 90°C, and 105°C). And second, air-cured at ambient temperature. After specimens were oven-dried at a specific temperature for 24 hours. Specimens were wrapped with polyethylene film until the experiment date was met. For sodium hydroxide solution molarity, four concentrations were used: 8 M, 10M, 12M, and 14M. These concentrations of alkaline liquid were used because they were reported to have high strength. The workflow of the experimental process in this study is shown in Figure 5.

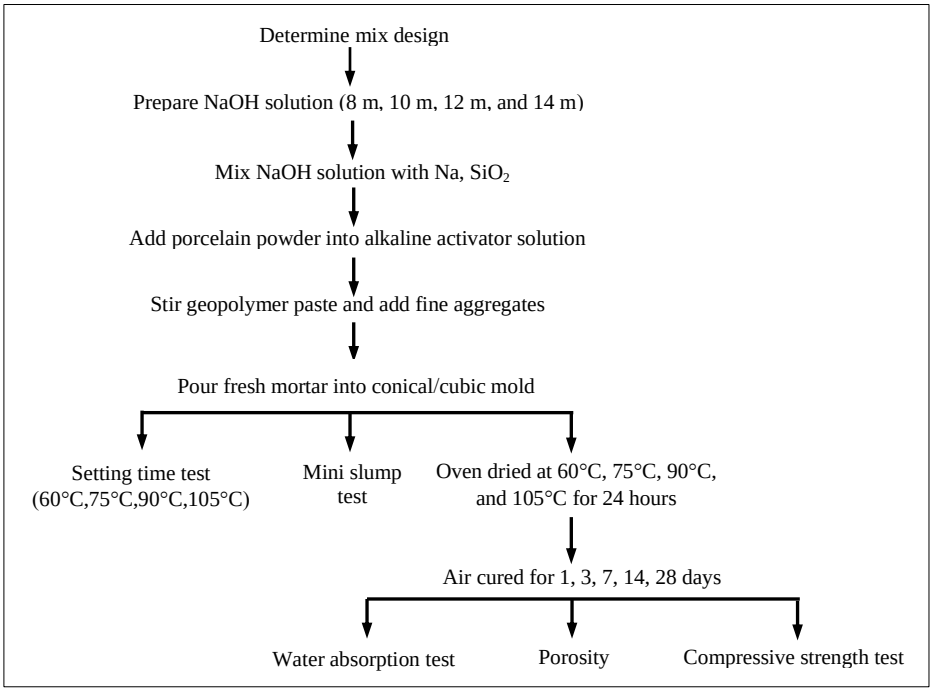

Figure 5. Schematic of process methodology

A flow table of the pastes was conducted by using a conical mold. The dimensions of the conical mold were 19 mm. in upper diameter, 38 mm. in diameter for the base, and a height of 57 mm. The porcelain geopolymer paste was poured into the mold and slowly lifted. The height was then measured. However, the workability test was started after 10 minutes when the dry mixture was mixed with the alkali-activated solution. The equation of flowability was given in Equation 1:

$$\text{Flow table } (\%) = \left(\frac{D_s - D_o}{D_o}\right) \times 100 \quad (1)$$

where D_s is diameter of specimen spread after test has done (mm), and D_o is diameter of specimen spread before test has started (mm).

Water absorption was made in accordance with ASTM C642 [32]. For the water absorption test, the cube specimens were fully dried in an air-dry oven at 105°C for 24 hours. The weight of the specimens was in grams (w_d). Before, when those specimens were fully immersed in still water for 24 hours and weighted repeatedly (w_s), the values of fully saturated and complete dry weight could be obtained. The water absorption (WA) was calculated using Equation 2 [33]. The classification of specimens was according to their water absorption capacity. Using EN ISO 10545 standard classification [34, 35], the level of water absorption could be categorized into three levels. Low water absorption: 0%≤WA≤0.5%, medium water absorption: 0.5%≤WA≤10.0% and high water absorption: WA>10%.

$$\text{Water absorption (WA,\%)} = \left(\frac{w_s - w_d}{w_d}\right) \times 100 \quad (2)$$

where W_s is weight before oven drying (g), W_d is weight after oven drying (g).

The porosity test was a guideline to indicate the effect of additives that had been added. The porosity of geopolymer concrete plays an important role in strength, permeability, and the long-term effect of durability in geopolymer concrete. The porosity of the specimens was then examined. The cube (50×50×50 mm) specimens were tested at different ages. The testing ages were 3, 7, 28, and 60 days. The specimens were placed in a vacuum-filled glass desiccator. The air was withdrawn from the desiccator and continued for 3 hours. Stilled water was introduced to the level that submerged the

specimens. The process of depressurization was repeated for three hours. Immediately after specimens were depressurized with stilled water, they were placed on a weight scale to measure their masses. After the porosity test, the saturated specimens were then oven-dried at 105°C for 72 hours. This helped to remove all the moisture from specimens and reweight oven-dried specimens repeatedly in air conditioning. The equation governing the porosity test was given in Equation 3.

$$\text{Porosity } (\%) = \left(\frac{m_{a(sat)} - m_{a(dry)}}{m_{a(sat)} - m_{w(sat)}}\right) \times 100 \quad (3)$$

where $m_{a(sat)}$ is Mass of saturated specimens in air (g), $m_{w(sat)}$ is Mass of saturated specimen in water (g), and $m_{a(dry)}$ = Mass of oven-dried specimens in air (g).

Initial and final setting times of porcelain with and without superplasticizer paste were investigated according to ASTM C191 using Vicat needles [36]. The specimens were placed into the oven for curing at the required temperatures of 60°C, 75°C, 95°C, and 105°C. Every 10 minutes, specimens were taken out for testing and immediately returned to the oven. The initial setting time test was carried out using a 1 mm-diameter needle. The depth of penetration was repeatedly recorded until the penetration of the needle reached 25 mm in depth or less. The final setting time was then determined when a 5-mm-diameter needle could not penetrate into the paste.

The strength of the specimen was subjected to compression. The compressive strengths of mortar were evaluated on a cube (50×50×50 mm). The strength of the specimens was tested and recorded by the Universal Machine (maximum load of 150 kN). The curing ages of the specimens were 3, 7, 14, and 28 days.

2.3. Mix Design

Mix design geopolymer mortar: The mixture proportion of porcelain-based geopolymer specimens was calculated:

1) AAS content and air fix AAS content: 550 kg/m^3 with assuming air 3%
2) $\frac{\text{AAS}}{\text{Binder}}$ = 0.7 with concentration of NaOH = 12M

   (2.1) $\frac{Na_2SiO_3}{NaOH}$ =2.50

   $NaOH = \frac{\text{AAS Content} \times \frac{\text{AAS}}{\text{Binder ratio}}}{3.5}$ =110 kg/m^3

   Na_2SiO_3 = NaOH content × 2.5 =275 kg/m^3

)2.2) Water content

   Solid content in NaOH = 48.5%

   Water content in NaOH = 110)1-0.485) = 56.6 kg/m^3

   Therefore, Solid content in NaOH =110-56.6 = 53.4 kg/m^3

   Water content in Na_2SiO_3 Solution = $275 \times \frac{50}{100}$ = 137.5 kg/m^3

   Total Water content = 56.6+137.5 = 194.1 kg/m^3
3) Determination of Total Aggregates :$V_{TA} 1 - \frac{3}{100} - \left(\frac{550}{2.7} + \frac{110}{1.4} + \frac{275}{1.56}\right) \times \frac{1}{1000}$ = 0.5 m^3
4) Calculation of fine and aggregates: Mass of fine aggregate MFA = 0.5×2.6×1,000 =1,328.6 kg/m^3
5) Superplasticizer: Used at 0.5% of porcelain content =2.8 kg/m^3

3. Results and Discussions

3.1. Chemical Analysis

3.1.1. X-Ray Fluorescence Spectroscopy

Porcelain was ground and run through the XRF spectrometer. It found that porcelain has both lower number ratio of $\left(\frac{SiO_2}{Al_2O_3}\right)$ and the sum of CaO+Fe_2O_3 when was compared with OPC. The $\left(\frac{SiO_2}{Al_2O_3}\right)$ and the sum of CaO+Fe_2O_3 determines the compressive strength of geopolymer porcelain. It appeared that porcelain-based geopolymers have good compressive strength.

3.1.2. X-Ray Diffraction

The X-Ray diffraction patterns of porcelain showed quartz alpha (SiO_2) and mullite ($Al_6Si_2O_{13}$) amorphous phases. The characteristic high intensities at 2q values of porcelain were 16.5, 20.9, and 26.8, while the high-intensity of OPC

2q values were 29.7, 33.3, and 34.2, respectively. However, the intensity of the porcelain decreased after calcination and geopolymerization. This might be due to the amorphous phase, which was the main component after geopolymerization [37, 38].

3.2. Standard Consistency and Setting Time

3.2.1. Standard consistency and Workability

The standard consistency of paste and workability of porcelain-based geopolymer mortar were examined. In this study, superplasticizer was used at a level of 0.5%. It was found that the normal consistency of porcelain-based geopolymer paste with/without superplasticizer (sp) decreased when the concentration of alkaline liquid increased. The consistency of 8M, 10M, 12M, and 14M geopolymer paste was 48%, 45%, 43%, and 43%, respectively. The workability of porcelain-based geopolymer mortar decreased when the concentration of alkaline liquid increased (Table 3). However, the effect of adding superplasticizer increased the workability of 8M, 10M, 12M, and 14M flow table specimens by 31.37%, 30.39%, 28.92%, and 27.45%, respectively. The workability of mini-slump increased by 85%, 82%, 80%, and 71%, respectively (Figure 6). The effect of using superplasticizer was great in low-concentration alkaline solution specimens. Applying a 0.5% dosage of superplasticizer was found to be insufficient to produce flowability in a high concentration of alkaline solution. An additional superplasticizer was needed when the concentration of the alkaline solution increased. The decrease in workability was due to the setting time of porcelain-based geopolymer pastes. The values of workability were relatively low on both flow table and mini-slump specimens without superplasticizer. Similar results were also found in high-calcium geopolymer materials [39].

(a) (b) (c) (d)

Figure 6. Flowability and Slump of 14M (a), (b) and 8M specimens (c), (d)

Table 3. Workability of porcelain based geopolymer mortar

Concentration (M)	Flow table (%)		Mini-Slump (mm)	
	w/sp	without/sp	w/sp	without/sp
8	35.29	3.92	20	3
10	32.35	3.92	17	3
12	30.39	1.96	10	2
14	28.43	1.47	7	2

As far as workability was concerned, the porcelain-based geopolymer mixture paste required a lesser amount of superplasticizer than low-calcium fly ash [40], iron, and steel slag [41] binder. This might be due to the specific surface area of fly ash, iron, and steel slag particles being greater than porcelain particles. Although, considering the fact that fly ash particles were spherical in shape, the specific surface area had greater influence than the shape of the particle. In order to maintain desired workability, it was advisable to increase workability by increasing the fine materials. In addition, the porcelain particles had a straight, flaky, elongated shape with sharp edges and a rough surface texture when compared with cement or fly ash particles. Therefore, an increment of alkali solution or superplasticizer was required to attain standard consistency. The low workability of fresh specimens led to high porosity and low strength. However, it might be suitable for non-load-bearing applications that need lighter structures.

3.2.2. Initial and Final Setting Time

Setting time penetration of porcelain-based geopolymers at various curing temperatures is shown in Figure 7. The ambient temperature and relative humidity of the environment were in the range of 34°C±2 and 72% ±1 respectively. The initial and final setting times with curing temperatures at 60°C, 75°C, 90°C, and 105°C are shown in Table 4. It was found that the initial and final setting times of porcelain-based geopolymer paste decreased when NaOH solution molarity increased. This was due to an increasing NaOH molarity, which enhanced the dissolution rate of the

aluminosolicate precursors and stimulated the geopolymerization process [42]. Porcelain was a low-calcium material, which gave it a low rate of geopolymerization at an early age. This was attributed to the low reactivity of porcelain material, which required time to change from plasticity to solid state. In the case of a high concentration of NaOH solution molarity, it was found that porcelain-based geopolymer paste took longer to reach solidification state when compared with a low concentration of NaOH solution molarity. Therefore, heat was then required to stipulate the geopolymerization rate.

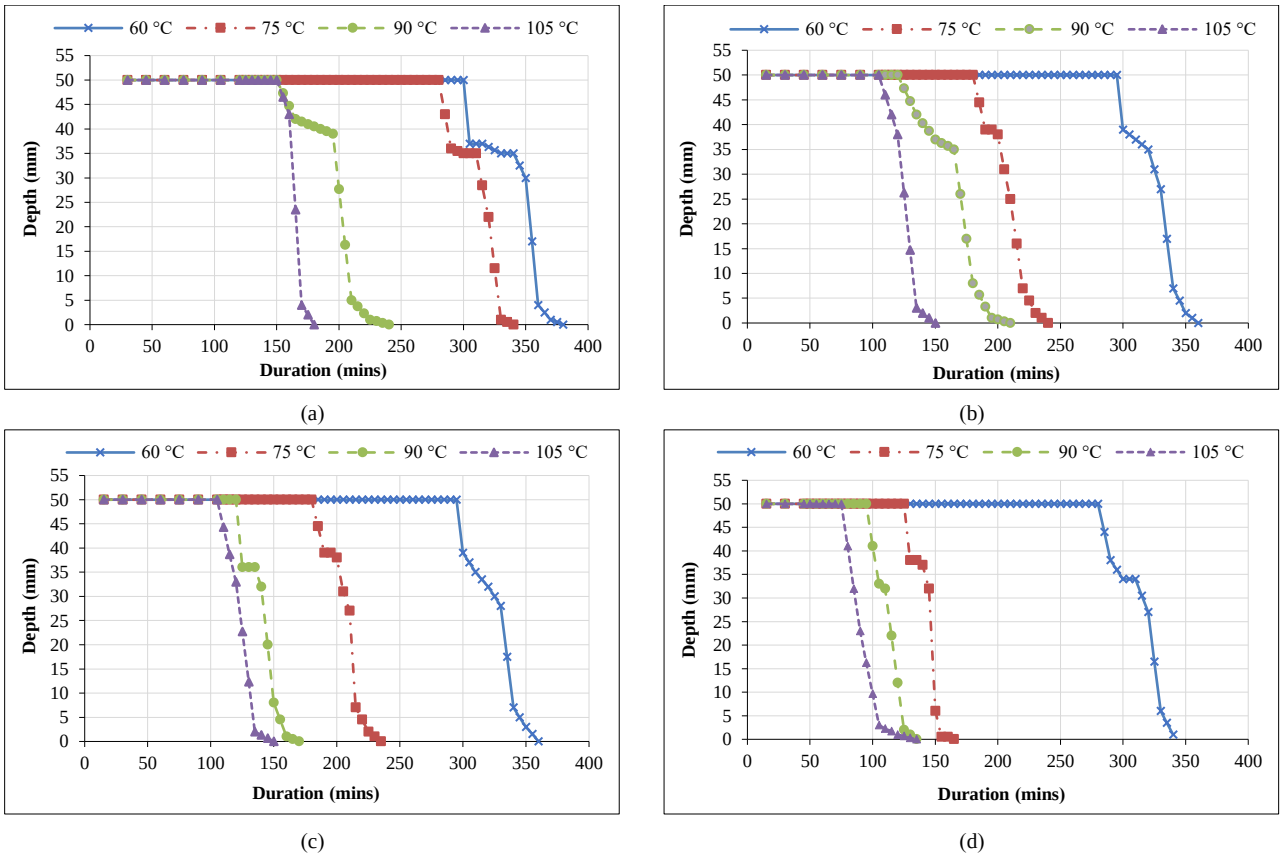

Figure 7. Effect of alkaline liquid concentration on setting time (a) 8 Molar (b) 10 Molar (c) 12 Molar (d) 14 Molar

Table 4. Setting time of specimens at various temperatures

Curing temp (°C)	Concentration (M)	Initial (mins)	Final (mins)
60	8	352	380
75	8	318	340
90	8	201	240
105	8	165	180
60	10	331	360
75	10	210	240
90	10	171	210
105	10	126	150
60	12	329	360
75	12	211	240
90	12	143	170
105	12	126	150
60	14	321	350
75	14	146	165
90	14	114	135
105	14	89	135

However, when applying heat to specimens, the rate of evaporation of water also increased as the curing temperature increased. This led to a higher concentration of the remaining alkali activator. In addition, the coverage of specimens also affected the rate of solidification. By opening the surface of specimens to expose curing heat. It accelerated the rate of evaporation of water, which increased the dissolution rate of aluninosilicate particles. Therefore, the rate of solidification of porcelain-based geopolymer paste depends on the initial curing temperature. The solidification of specimens started from surface to core. The hot air caused the surface of the specimens to harden while the internals were still soft.

In this study, the authors had not yet found a situation where an increase in NaOH solution molarity led to an increase in initial and final setting times. This behavior is usually found in high-calcium materials [43]. The influence of superplasticizer on the setting time of pastes had not been noticed. In general, penetration depth and setting time depended on the alkaline solution and its activator composition, which affected workability. It was also found that an increase in curing temperature stimulated the geopolymerization process. At low curing temperatures (60°C and 75°C), the geopolymer pastes set slowly. The initial and final setting times were longer than the other curing temperatures. A similar result was found by Liew et al. [44]. The 8M geopolymer paste reached its setting times (initial and final) at 352 minutes, 380 minutes, and 318 minutes, 340 minutes, respectively. While at high curing temperatures (90°C and 105°C), the initial and final setting times were 201 minutes, 240 minutes, 165 minutes, and 180 minutes, respectively. At 8 M, solidification of porcelain paste was noticed when porcelain-based geopolymer pastes reached 300 minutes (60°C and 75°C) and 180 minutes (90°C and 105°C). The effect of curing temperature on NaOH molarity was clearly pronounced when the concentration of alkaline liquid was above 8 molar and the temperature of curing was above 60°C. The setting time decreased when the curing temperature increased. Similar results were found in fly ash [45] and metakaolin [13, 46] based geopolymers. The high rate of setting was due to the temperature-controlled dissolution of aluminosilicate precursors that were reactive at high temperatures [47]. The characteristic setting time of porcelain powder mixed with alkaline liquid was found to be similar to that of other low-calcium geopolymer materials [48]. However, the concentration of alkaline liquid had a lesser effect on paste hardening than high-curing-temperature pastes. The geopolymerization process was easily stimulated when the concentration of alkaline liquids was high.

In addition, an increment in the concentration of alkaline liquid also caused less consistency in the paste, which led to less dissolution of the activator solution. For the effect of alkaline concentration on the geopolymerization process, it was found that the concentration of alkaline liquid affected the starting time of the second stage of the geopolymerization process. The starting time of the second stage of the geopolymerization process decreased as the concentration of alkaline liquid increased. At 10M or above, the concentration of alkaline liquid showed an obvious effect on the starting point of the second stage of the geopolymerization process. While, at 8M, a curing temperature above 75°C is required to stimulate the geopolymerization process. It could be noted that porcelain-based geopolymer mix activated with alkali solution decreased the final setting time, whereas fly ash type F and ground granulated blast furnace (GGBS)-based geopolymer paste increased the final setting time [49].

Table 5 shows the initial and final setting times of geopolymer mortar with different binders. It can be noticed that the initial and final setting times of fly ash mixes increased with calcium content. While ground granulated blast furnace slag (GGBS) was a cementitious material with a high calcium content. The setting time of the slag paste rapidly decreased. In this study, the setting time of porcelain-based geopolymer was acceptable when compared with other binder materials. From this study, the initial and final setting times of 12 M specimens at a curing temperature of 105°C were 89 minutes and 135 minutes, respectively. While fly ash, with 24 hours of oven drying at 110 °C, had initial and final setting times of 190 minutes and 230 minutes, The faster setting time of fly ash was due to the formation of micro-cracks on fly ash particles during rapid water escapement, which caused more reactive materials to enter the activation environment. The strength of the paste depended on the amount of aluninosilicate gel produced during the geopolymerization process [50]. The interface bonding between gel and fine aggregate was expected to have a significant bearing on the strength of geopolymer paste specimens. In order to increase the interface bonding, higher heat was required.

Table 5. Setting time and heat conditions of various binder materials based geopolymer

Binder	Heat treatment	Initial setting (min)	Final setting (min)	Particle size, d_{50} (μm)	Compressive strength (N/mm^2)
Fly ash [51]	1 hr. oven dried at 110 °C	170	220	12	70±3
Fly ash [51]	24 hrs. oven dried at 110 °C	190	230	12	73±3
Ferrochrome slag [52]	96 hrs. at 22 °C	235	870	< 43	1.52 (paste), curing at 80°C
50% Fly ash+35% GGBS+15% Silica Fume [53]	48 hrs. oven dried at 90 °C	40	110	< 45	31
50% Fly ash+ 50% GGBS [53]	48 hrs. oven dried at 90 °C	20	65	< 45	28

3.3. Absorption and Porosity

The water absorption and porosity of porcelain-based geopolymers were studied (Figure 8). All cube specimens were oven-dried at 60°C, 75°C, 90°C, and 105°C for 24 hours. The air curing temperature was ambient temperature (35-37°C). According to the findings, the absorption of specimens showed the large voids contained within specimens, while the porosity showed the capillary small voids. The water absorption of all specimens was high in the early curing ages, regardless of curing temperature, oven-drying time and air curing time. Table 6 shows that the rate of absorption gradually improved after specimens reached saturation level. The initial rate of water absorption decreased as the concentration of alkaline liquid increased. The decrease in water absorption was noticed at 3, 7, 14, and 28 days. It was found that specimens at day 28 showed the lowest percentage of water absorption and porosity, whereas specimens at day 1 showed the highest water absorption and porosity.

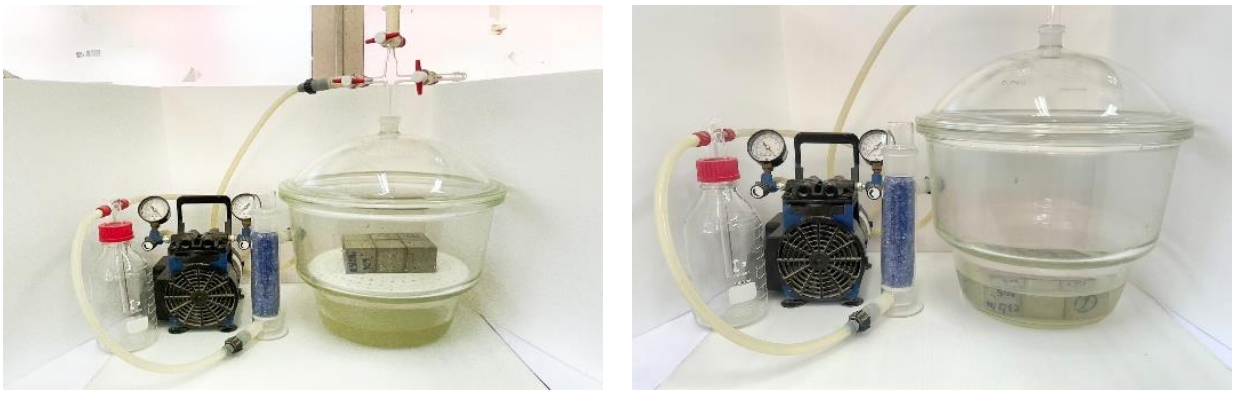

(a) (b)

Figure 8. Porosity test (a) De-aired (b) Fully submerged specimens

Table 6. Absorption of specimens at various curing days

Concentration (M)	24 hrs. oven-drying temp (°C)	Absorption (%)				
		Air-cured (days)				
		1	3	7	14	28
14	60	12.8	12.1	11.6	11.3	11.1
14	75	10.9	10.7	10.3	10.1	9.9
14	90	9.8	9.5	9.1	8.9	8.5
14	105	7.8	7.4	7.1	6.9	6.6
12	60	14.9	14.1	13.7	13.1	12.7
12	75	13.0	12.6	12.1	11.4	10.6
12	90	10.1	9.9	9.4	9.0	8.8
12	105	8.3	7.7	7.4	7.1	6.9
10	60	19.1	18.4	18.2	18.0	17.6
10	75	16.0	15.1	14.6	14.0	13.0
10	90	13.2	12.8	12.1	11.6	10.8
10	105	9.2	8.8	8.4	8.3	7.9
8	60	19.3	18.8	18.5	18.2	17.5
8	75	16.0	15.1	14.6	14.0	13.0
8	90	13.2	12.8	12.1	11.6	10.1
8	105	9.2	9.0	8.4	8.3	8.1

A higher water absorption value at early curing age could be attributed to the existence of larger voids, while a lower water absorption value might be ascribed to the formation of geopolymerization products in the microstructure [54]. The internal structure of specimens became denser and improved crystallinity from day 1 onward. The formation of a well-compressed microstructure led to fewer vacancies. Similar results were found by Olivia & Nikraz [55], Lavanya & Jegan [56], and Zaidi et al. [57]. The porosity of specimens was affected by the pore structure of the specimens, which depended on the concentration of alkaline solution, the duration of submersion in still water with the porosity test, and the duration of curing in oven dry before specimens were subjected to the porosity test.

Addition, Figures 9a and 9b show the characteristic surfaces of 8M and 14M specimens with oven curing at 105°C, respectively. The number and size of pores decreased when the concentration of alkaline liquid increased. The rate of absorption rapidly decreased during the first 3 days. It appeared that the geopolymerization process of porcelain powder had better reacted with higher temperatures and higher alkaline concentrations. The results also confirmed the setting time test results. The pore size decreased, and the structure became denser. The porosity and permeability of the specimens decreased. The durability of specimens could potentially be expected.

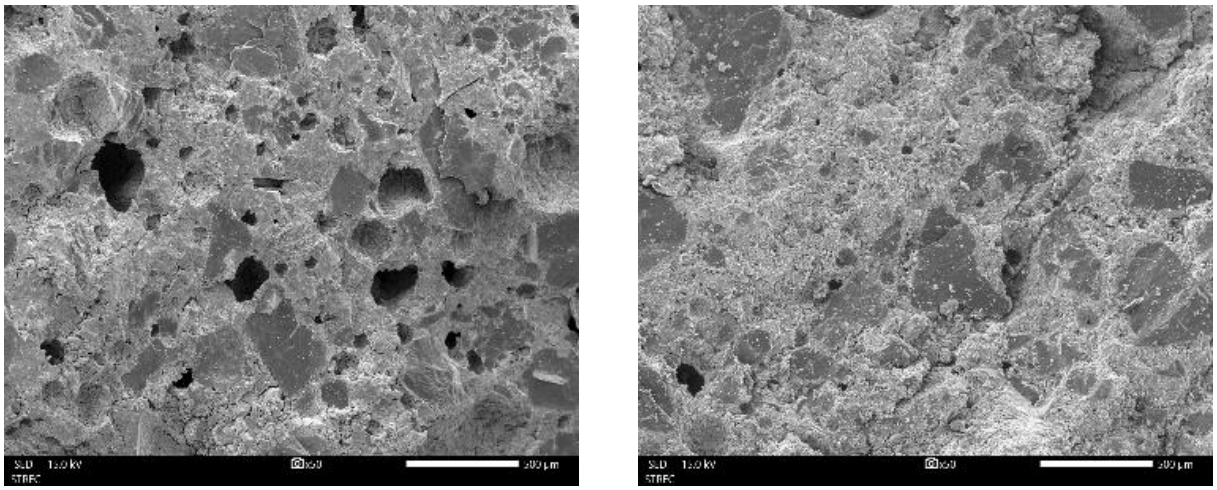

(a) (b)

Figure 9. Surface of specimens at difference curing age (a) Surface of specimens at 8M with 28 days curing (b) Surface of specimens at 14M with 28 days curing

Figure 10 shows the porosity of specimens at various concentrations after 24 hours of oven-curing temperatures. The characteristic of porosity was similar to the water absorption results. The 1-day-old specimens had difficulty measuring the weight of ingress water because they were still gelatinous and moist, which meant they might easily break from their original shape during the weight measurement. Especially the high NaOH concentrations (12M and 14M) and 60°C curing temperatures required extra time to measure the weight. The absorption rate decreased when alkaline concentrations increased. Even specimens had dissolution of alkaline liquid while submerged in desiccator water. In contrast, other works showed that slag mixed with low-calcium fly ash [58] and low-calcium fly ash mixed with steel fiber-reinforced geopolymer concrete [59] required less time to solidification.

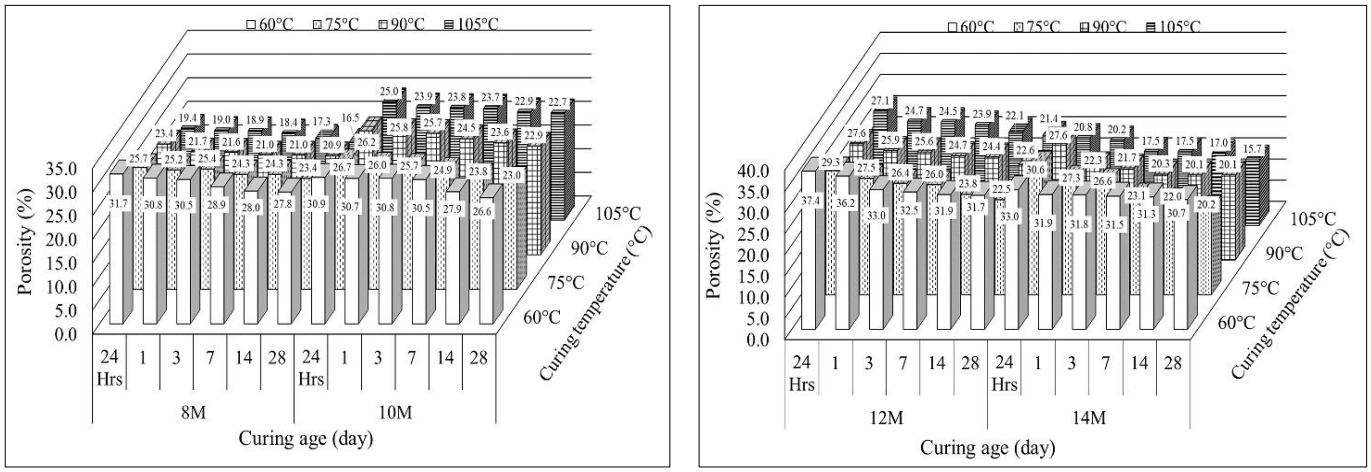

(a) (b)

Figure 10. Porosity of specimens at various temperature (a) 8M and 10M (b) 10M and 12M

For the effect of curing temperature, an increment of 15°C from 60°C to 75°C had the highest effect on reducing the porosity of specimens. At 28 days into the curing period, the rate of decrease in porosity was 0.70%/°C. while increments of temperature from 75°C to 90°C and 90°C to 105°C had a lesser rate of decreasing porosity values of 0.05%/°C and 0.29%/°C, respectively. Overall, specimens with an initial curing temperature of 105°C had the lowest porosity value when each alkaline concentration level was compared. An increment in alkaline concentration influenced both non-reacted and partly reacted particles, which led to an added porous structure. However, all specimens were subjected to 24 hours of oven-dry curing, which helped advance the geopolymerization process and dry the specimens. It found that 28-day air-cured specimens with an 8M concentration had the highest water absorption (17.5%), while the lowest water

absorption was found in 28-day air-cured specimens with a 14M alkaline concentration (6.5%). It was noticeable that the water absorption decreased with increasing cure time. However, the rate of absorption gradually decreased with time since pores had gradually filled with geopolymerization products.

The higher temperature and longer curing period in oven resulted in rapid evaporation and heavy loss of water from pores. Larger pores were highly prone. An increasing volume of open pores by high curing temperatures increased porosity of geopolymer mixed with ceramics specimens. The percentage of porosity continuously increased with curing temperature and time [60]. An increase in percentage of high alkali concentration specimens which were subjected to high curing temperature, were not found in this study. An increment of internal surface area of pores was influenced by temperature and period of curing. The lowest porosity achieved with activator solution 14M when specimens were subjected to 24 hours oven-cured and 28 days air-cured (15.7%). It was also found that the relationship between absorption and porosity of specimens was exponential behavior as absorption increased porosity of specimens increased with decreasing in temperature of drying oven. The decreasing in water adsorption rate had been noticed since 1day air-cured age (Figure 11).

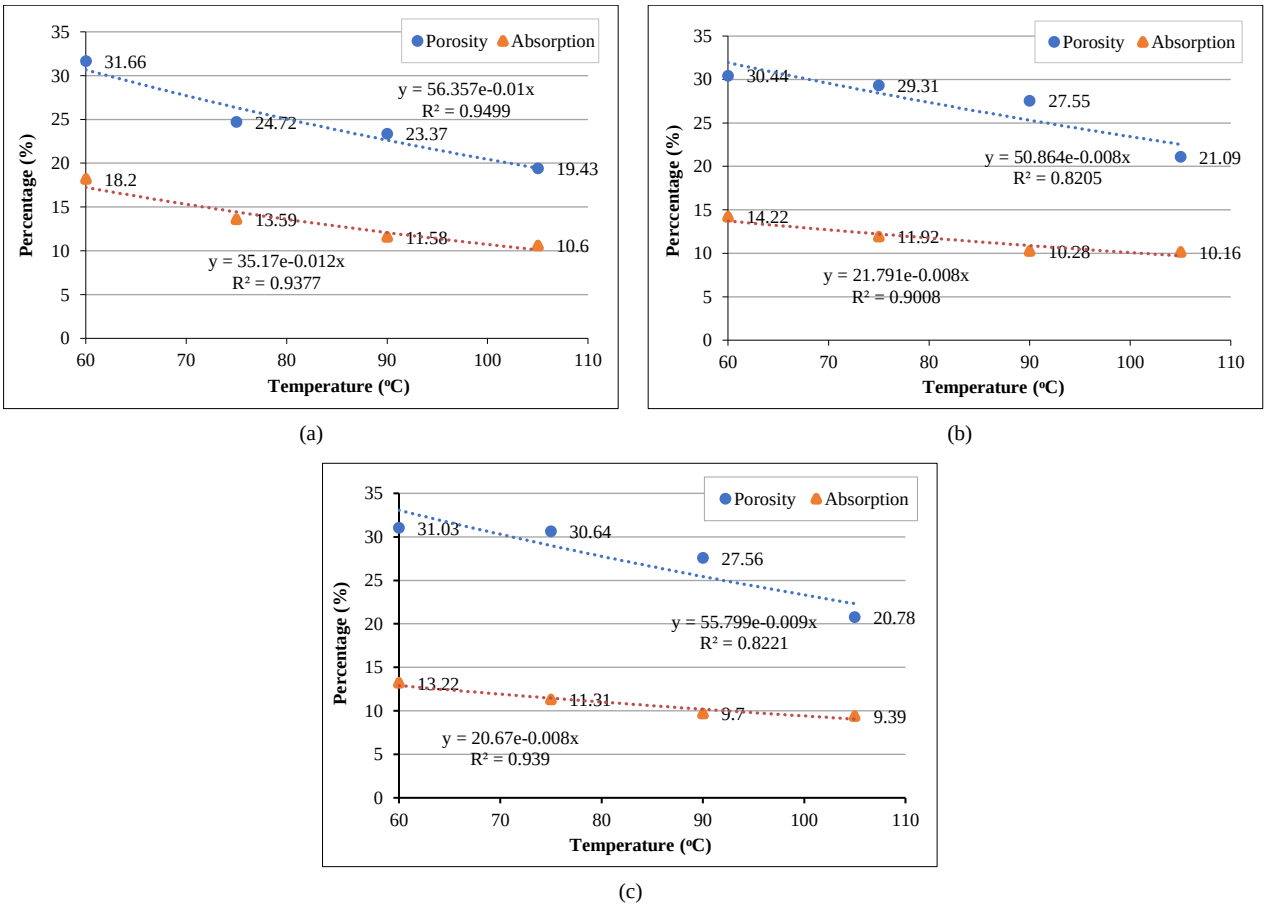

Figure 11. Correlation between porosity and absorption at 1 day age various curing temperature (a) 8M (b)-12M (c) 14M

This was due to solidification of internal structure of specimens which led to denser and harder. The product (crystalline) of alkaline solution mixed with activator was developed. The durability and permeability of specimens had been improved with time. Similar results were also found toward the temperature of drying oven. Heat was required in development of internal structure. The relationship between water absorption and porosity decreased exponentially with a relative high correlation coefficient (R^2). It showed that specimens with higher water absorption and porosity were potentially less durable. As far as porosity and absorption were concerned, the effectiveness of porcelain powder used as binding material could be insighted. The rate of decreasing porosity and voids in specimens were similar to low calcium fly ash material and slag [60].

3.4. Development of Strength

3.4.1. Curing Temperature and Curing Period

The compressive strength test was performed by taking three specimens from each set after 3, 7, 14, and 28 hours of curing in air. Figure 12 shows the failure of compressive specimens at various curing temperatures. The compressive strength results are shown in Figure 13. The compressive strength increased with the increase in concentration of NaOH

from 8M to 14M. However, oven-dry curing time was further extended from 2 hours to 24 hours. The two, four, six, and eight-hour periods in the oven were not long enough to make ready-to-test specimens. The specimens were still moist and soft. The compressive strength of the specimens was lower. Comparably, the specimens were oven-cured at 75 °C, 90 °C, and 105 °C, which showed a faster increase in compressive strength. A similar result was found by Mo et al. [13]. This was due to the slow dissolution of porcelain particles. The geopolymerization products grew slowly. The amounts of precursors dissolved from amorphous phases in porcelain were insufficient to polymerize with amorphous Si precursors in activators to form enough aluminosilicate gels. As a result, a plentiful amount of sol phase and water were in the system, which caused the value of compressive strength to be lower than that of specimens cured at a higher temperature. It was found that the length of drying in the oven and curing in the air influenced the hardening of specimens. The 24-hour oven-dry specimens were then preferred. The specimens were denser and harder. The compressive strength of sanitary ware porcelain based geopolymer mortar increased with time and concentration of NaOH. High temperatures in oven-dry curing with a short curing time enhanced both the solidification of specimens and the development of compressive strength [61, 62].

The rate of increase in strength was significantly noticed when specimens were initially heated from 75°C upward for 24 hours. It was widely understood that curing geopolymer at a higher curing temperature resulted in increased early strength while having a negative effect on the final strength of the material. Curing temperature from 60 °C to 105°C, the compressive strength increased with curing temperature. The adverse effect on the final strength was not found when compared with metaokaolin [13, 63] and fly ash [64, 65]-based geopolymers. This was due to the low calcium content of porcelain. At high curing temperatures, dissolution and condensation occurred at a rapid rate. However, the rate of condensation was slower than that of metakaolin and fly ash. Plenty of reactive materials were generated to condense. The geopolymerization process caused reactive aluminosilicate particles to largely remain in the system. Therefore, the dissolution and condensation processes of unreactive particles could continue over time. However, the rate of increase in compressive force declined with time. This was due to the availability of aluminosilicate particles and the accessibility of solvent to the inner layers of aluminosilicate particles. The particles were obstructed by the formation of geopolymerization gel products that surrounded aluminosilicate particles. Prolonging oven-dry time was not advisable. An excessive drying oven period caused further moisture escapement through cracks and voids, which led to the shrinkage of specimens. With an appropriate period of curing time and drying oven temperature (105°C), the continual dissolution of porcelain powders was very fast, which helped to promote fast polymerization to form geopolymer gels and transformation into hard structures [40].

Figure 14 shows the formation of cracks on the surface of specimens. The formation and number of crack lines were greater and deeper in low-concentration alkaline solution specimens. The occurrence of cracks rapidly increased when high concentrations of alkaline specimens were cured for an excessive 24 hours. A similar result was also found when specimens with high alkaline concentrations were oven-dried at a high temperature. In this study, microcracks with discontinuous gel did not appear on the specimens after they were oven-cured. However, under microscopic, micro cracks were mostly found in low alkali concentration with early age of curing specimens. While, large cracks were identified in the other ceramic-based geopolymer mortar specimens following immersion in water [66]. It was due to the inclusion of calcium silicate hydrate phases that provided stiffness to the geopolymer specimens, improving the mechanical properties of porcelain-based geopolymers. The formation of early-age cracking also depended on the development of strength in specimens.

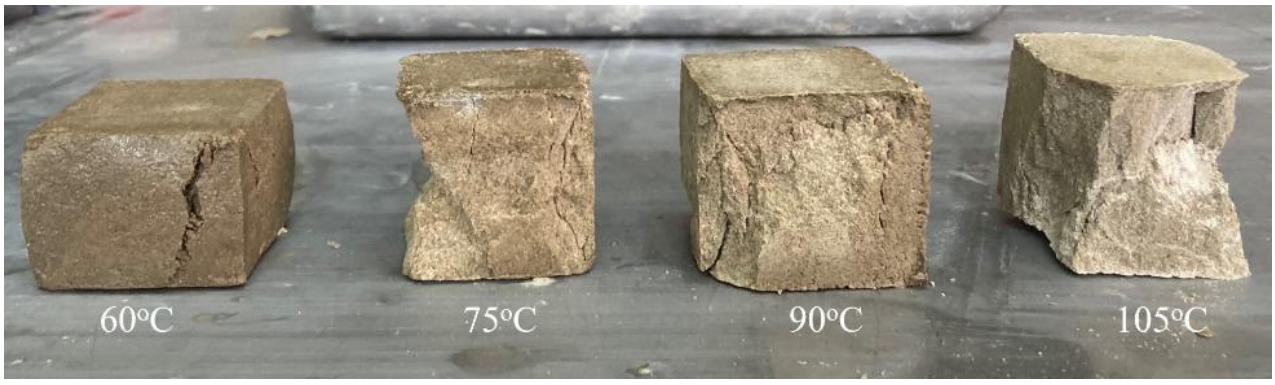

Figure 12. Typical 28 days curing age specimens' failure under compressive strength test

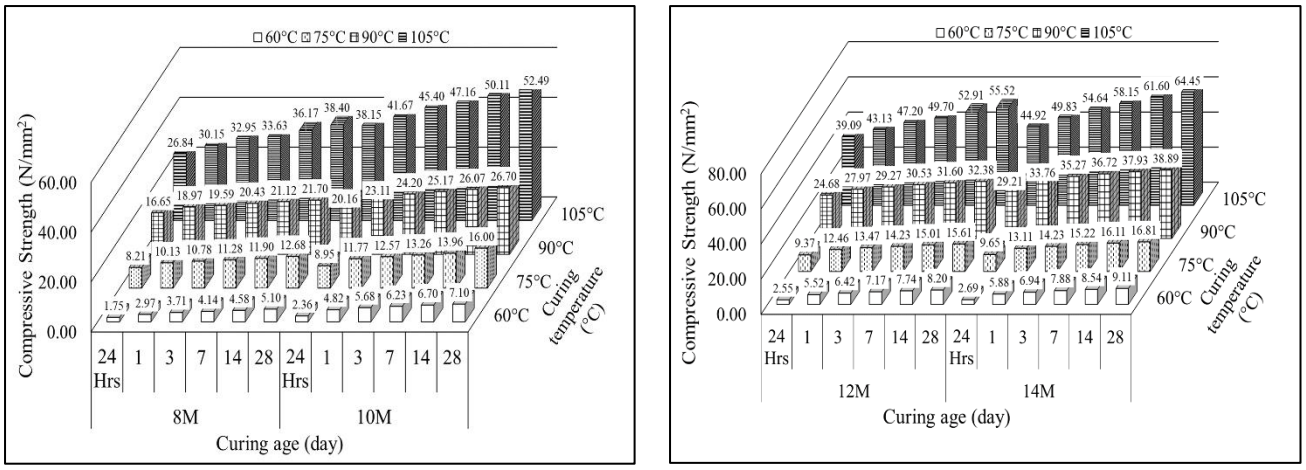

(a) (b)

Figure 13. Compressive strength at various temperature and period of curing (a) 8M and 10M (b) 12M and 14M

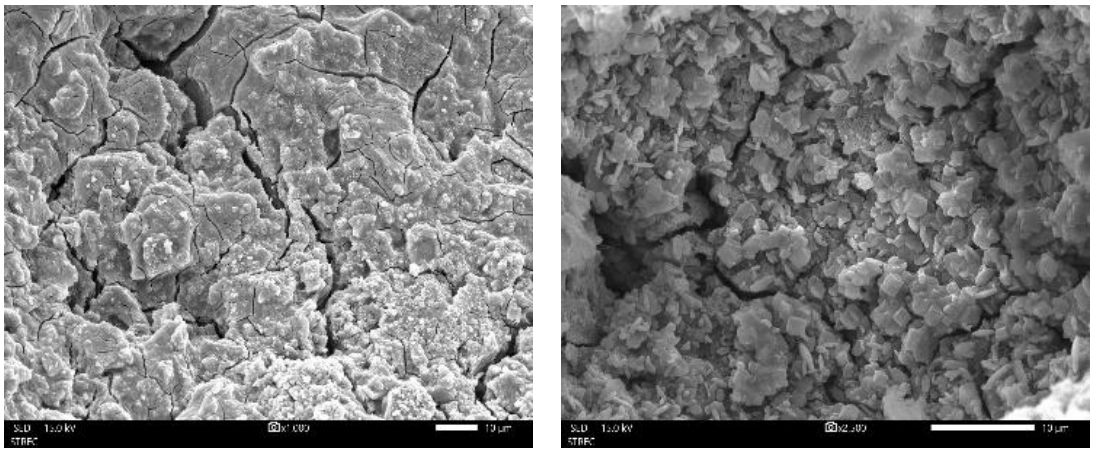

(a) (b)

Figure 14. (a) Characteristic of crack on surface of 8M with 28 days curing specimen (b) Characteristic of cracks on surface of specimens at 14M with 28 days curing

The overheating temperature was usually considered to be above 105°C. By applying an excessive curing duration and a high conventional curing temperature (105°C), it could harm the physical and mechanical properties of specimens. The crack lines might cause the strength of specimens to decrease as the concentration of alkaline solution increased. It might relate to the de-bonding between geopolymer materials, which held particles together were weak. The porcelain particles were mainly bonded by chemical bonding. The severe escapement of moisture and shrinkage of specimens occurred when high temperatures and a long period of oven-curing conditions were introduced. The development of cracks mainly occurred within the 24-hour oven-drying period. Therefore, an appropriate length of drying oven and a suitable temperature for curing should be taken into consideration. For the effect of curing temperature on the development of compressive strength, the rate of increase in strength was not steady. The specimens with the fastest rate of increase in strength had 14M specimens with a curing temperature of 105°C.

The strength of specimens increased at 0.70 N/mm^2 per day. While the 8M specimens with a curing temperature of 60°C gained strength at a rate of 0.12 N/mm^2 per day. It was found that both curing temperature and curing period had an effect on the increment of porcelain-based geopolymer mortar strength. However, it appeared that the sensitivity of curing temperature to strength was higher than curing time. In addition, porcelain material was a slow-reacting material when compared with low-calcium fly ash and slag. The geopolymerization process of porcelain binder was then slower than that of low-calcium fly ash and slag [67]. The increment of strength from 1 to 7 days was significantly higher than the increment of strength during the 7 to 28-day period. This was due to the availability of calcium hydroxide and calcium silicate to react with the porcelain binder. The formation of calcium aluminosilicate and geopolymerization products (calcium silicate hydrate) rapidly occurred during the geopolmerization process [68]. The results showed that as the concentration of alkaline solution increased, the initial and ultimate strengths increased significantly. This indicated that the aluminosilicate source underwent further dissolution, which led to its chemical structure changing [52, 69]. It appeared that the porcelain powder had a good response to an alkaline solution. The concentration of alkaline solution had a significant effect on the strength of porcelain-based geopolymer mortar.

However, an appropriate drying oven at a high temperature was also needed to achieve the desired strength. The strength of porcelain-based geopolymer mortar increased with time once specimens were initially cured by heat. At ambient temperatures, a heating system was required to provide heat to the geopolymer members when the formwork had been removed. Thus, individual work required a specific initial heat-curing temperature and duration to fit the needs of practical application. Table 7 shows that the compressive strength of a geopolymer depends on several factors from prior studies. These factors included binding materials and curing methods. However, curing at an elevated temperature above 60 °C for more than 24 hours appeared to promote the development of compressive strength. It appeared that curing specimens above 75°C increased the compressive strength significantly. In this study, it was found that introducing porcelain as a binding material gave reasonable high compressive strength when compared with calcined kaolinite claystone (68 N/mm^2) [66] and kaolin (19.83–48 N/mm^2) [67, 68]. Selecting a suitable water glass type of alkali activator also enhanced the mechanical properties of the geopolymer mortar used, as porcelain has good compressive strength. However, the state of the material (liquid or solid) also affected compressive strength due to phase and bond formation in the geopolymerization process.

Table 7. Compressive strength and binding material used

Reference	Binding materials	Curing method	Compressive strength	Activator
Hájková (2018) [70]	Calcined kaolinite claystone	Ambient, oven dry, microwave	68 N/mm^2 at 28 days curing	Sodium silicate, sodium hydroxide
Matalkah et al. (2020) [71]	Kaolin	Heat and ambient curing	48 N/mm^2	Potassium silicate and calcium hydroxide
Ababneh et al. (2020) [50]	Kaolin	Heat and ambient curing	7-day 19.83 N/mm^2 (heat cure) 16.47 N/mm^2 (room-cure)	Sodium silicate, sodium carbonate, calcium oxide

4. Conclusions

The mechanical properties of sanitary ware porcelain powder used as binder material for geopolymer were discussed concerning four principal characteristics (consistency, setting time, porosity, and compressive). This research found that the consistency of 8M, 10M, 12M, and 14M porcelain-based geopolymer paste was 48%, 45%, 43%, and 43%, respectively. The setting times and workability of the porcelain-based geopolymer paste increased when the concentration of NaOH molarity decreased. An increasing alkaline concentration decreased the overall viscosity of porcelain-based geopolymers. Thus, mixing for a longer period was not advisable. The rapid clotting of the geopolymer slurries caused the undissolved porcelain particles to be covered with geopolymer gel. Extra attention should be paid when the curing temperature is between 90°C and 105°C, the viscosity of geopolymerization products increases rapidly at the onset of polycondensation. The initial and final setting times rapidly decreased. An excessive curing time and overly high temperature caused microcracks and contraction in geopolymer specimens. Hence, full coverage of the specimen during oven curing should be applied. Otherwise, dehydration, excessive moisture loss, and shrinkage at high temperatures occurred. In addition, the efficiency and potentialities of compaction were also affected. Voids and capillary pores. Superplasticizer was then needed to increase the workability of pastes. The alkali concentration level had an obvious effect on the final setting time. By increasing the alkali concentration level, the final setting time decreased. The setting time of porcelain-based geopolymer paste at low curing temperatures (60°C and 75°C) sets slowly. Therefore, the solidification of specimens required time.

From the SEM analysis, lower alkaline concentrations caused the unreacted porcelain particles. In addition, prolonged curing periods in oven-dry with high temperatures caused internal crack lines in low alkaline-concentration porcelain-based geopolymer mortar.

The research found that increasing the length of the drying oven decreased porosity and water absorption rate. The capillary voids of the specimen decreased as the concentration of alkaline solution increased. The optimal alkaline concentration of the porcelain-based geopolymer mortar was 14M when cured for 24 hours at 105°C. This governed condition provided the lesser value in water absorption and porosity of porcelain-based geopolymer mortar. The sanitary ware porcelain had potential to be used as an alternative binder for geopolymer products. Although porcelain-based geopolymer mortar could be cured at ambient temperature, heat curing was recommended. Hot air curing helped complete the chemical reaction in the geopolymerization process.

The compressive strength of porcelain-based geopolymer mortar was influenced by the constituent binder materials that make the geopolymer paste. The test results also showed that higher concentrations (molar concentrations) of sodium hydroxide solution enhanced the compressive strength of geopolymer mortar. In addition, the compressive strength increased as pores decreased. The ultimate compressive strength was 64.45 kN/mm^2 for 28 days of air curing. The rapid rate of increase in compressive strength occurred during 7 days of curing in air. The compressive strength increased with an increase in alkaline concentration. The rate of increase in strength increased as the alkaline concentration increased. Therefore, the specimens with higher alkaline concentrations had lesser water absorption and porosity values. Hence, the permeability of ingress water was reduced. The durability of porcelain-based geopolymer mortar was also improved.

For sanitary ware porcelain powder-based geopolymer mortar, a definite mix design was not clearly available in the past literature, which was incorporated into the present work. Trials and errors were conducted to seek an appropriate mix proportion. However, the addition of a naphthalene sulfonate-based superplasticizer dosage greater than 0.5% resulted in higher flowability and viscosity of the geopolymer paste. The viscosity of the geopolymer paste rapidly decreased with time. Therefore, speed and enormous energy for placing and compacting were needed for producing geopolymer mortar specimens.

5. Declarations

5.1. Author Contributions

Conceptualization, B.I.N.A.; methodology, B.I.N.A.; validation, B.I.N.A.; formal analysis, B.I.N.A.; investigation, W.W.; resources, B.I.N.A.; data curation, B.I.N.A.; writing—original draft preparation, W.W. and B.I.N.A.; writing—review and editing, B.I.N.A.; visualization, B.I.N.A.; supervision, B.I.N.A.; project administration, B.I.N.A.; funding acquisition, B.I.N.A. All authors have read and agreed to the published version of the manuscript.

5.2. Data Availability Statement

The data presented in this study are available on request from the corresponding author.

5.3. Funding

Rajamangala University of Technology Thanyaburi (FRB65E0707J.4), Grant Recipient: Borvorn Israngkura Na Ayudhya.

5.4. Acknowledgements

The authors are greateful to the Rajamangala University of Technology Thanyaburi for supportion this study through Project “A study of physical properties of porcelain powder used for geopolymer concrete sleeper in depot (FRB65E0707J.4)”.

5.5. Conflicts of Interest

The authors declare no conflict of interest.

6. References

[1] Statista. (2022) Construction industry in Thailand. Statista Research Department, Hamburg, Germany. Available online: https://www.statista.com/topics/6998/construction-industry-in-thailand/#topicOverview (accessed on May 2023)

[2] Baraldi, L. (2021) World sanitaryware imports and exports, Ceramic world review technology news markets, 64-75. Available online: https://www.ceramicworldweb.com/en/economics-and-markets/world-sanitaryware-imports-and-exports-2021 (accessed on April 2023).

[3] Zuda, L., Bayer, P., Rovnaník, P., & Černý, R. (2008). Mechanical and hydric properties of alkali-activated aluminosilicate composite with electrical porcelain aggregates. Cement and Concrete Composites, 30(4), 266–273. doi:10.1016/j.cemconcomp.2007.11.003.

[4] Fortuna, A., Fortuna, D.M., Martini, E. (2017). An Industrial Approach to Ceramics: Sanitaryware. Plinius, 43, 138–145. doi:10.19276/plinius.2017.02019.

[5] Nasir, M., Johari, M. A. M., Maslehuddin, M., Yusuf, M. O., & Al-Harthi, M. A. (2020). Influence of heat curing period and temperature on the strength of silico-manganese fume-blast furnace slag-based alkali-activated mortar. Construction and Building Materials, 251, 118961. doi:10.1016/j.conbuildmat.2020.118961.

[6] Muñiz-Villarreal, M. S., Manzano-Ramírez, A., Sampieri-Bulbarela, S., Gasca-Tirado, J. R., Reyes-Araiza, J. L., Rubio-Ávalos, J. C., Pérez-Bueno, J. J., Apatiga, L. M., Zaldivar-Cadena, A., & Amigó-Borrás, V. (2011). The effect of temperature on the geopolymerization process of a metakaolin-based geopolymer. Materials Letters, 65(6), 995–998. doi:10.1016/j.matlet.2010.12.049.

[7] Hardjito, D., & Rangan, B. V. (2005). Development and properties of low-calcium fly ash-based geopolymer concrete. Research Report GC1, Curtin University of Technology, Perth, Australia.

[8] Provis, J. L., & Van Deventer, J. S. J. (2009). Geopolymers: structures, processing, properties and industrial applications. Elsevier, Amsterdam, Netherlands.

[9] Arnoult, M., Perronnet, M., Autef, A., & Rossignol, S. (2018). How to control the geopolymer setting time with the alkaline silicate solution. Journal of Non-Crystalline Solids, 495(1), 59–66. doi:10.1016/j.jnoncrysol.2018.02.036.

[10] Luhar, I., Luhar, S., Abdullah, M. M. A. B., Nabiałek, M., Sandu, A. V., Szmidla, J., Jurczyńska, A., Razak, R. A., Aziz, I. H. A., Jamil, N. H., & Deraman, L. M. (2021). Assessment of the suitability of ceramic waste in geopolymer composites: An appraisal. Materials, 14(12), 3279. doi:10.3390/ma14123279.

[11] Shoaei, P., Musaeei, H. R., Mirlohi, F., Narimani zamanabadi, S., Ameri, F., & Bahrami, N. (2019). Waste ceramic powder-based geopolymer mortars: Effect of curing temperature and alkaline solution-to-binder ratio. Construction and Building Materials, 227, 116686. doi:10.1016/j.conbuildmat.2019.116686.

[12] Reig, L., Tashima, M. M., Soriano, L., Borrachero, M. V., Monzó, J., & Payá, J. (2013). Alkaline activation of ceramic waste materials. Waste and Biomass Valorization, 4(4), 729–736. doi:10.1007/s12649-013-9197-z.

[13] Mo, B. H., Zhu, H., Cui, X. M., He, Y., & Gong, S. Y. (2014). Effect of curing temperature on geopolymerization of metakaolin-based geopolymers. Applied Clay Science, 99, 144–148. doi:10.1016/j.clay.2014.06.024.

[14] Nagral, M. R., Ostwal, T., & Chitawadagi, M. V. (2014) Effect of curing temperature and curing hours on the properties of geo-polymer concrete, International Journal of Computational Engineering Research. 4(9), 2250-3005.

[15] Duxson, P., Fernández-Jiménez, A., Provis, J. L., Lukey, G. C., Palomo, A., & Van Deventer, J. S. J. (2007). Geopolymer technology: The current state of the art. Journal of Materials Science, 42(9), 2917–2933. doi:10.1007/s10853-006-0637-z.

[16] de Oliveira, L. B., de Azevedo, A. R. G., Marvila, M. T., Pereira, E. C., Fediuk, R., & Vieira, C. M. F. (2022). Durability of geopolymers with industrial waste. Case Studies in Construction Materials, 16, 839. doi:10.1016/j.cscm.2021.e00839.

[17] Kaur, M., Singh, J., & Kaur, M. (2018). Microstructure and strength development of fly ash-based geopolymer mortar: Role of nano-metakaolin. Construction and Building Materials, 190, 672–679. doi:10.1016/j.conbuildmat.2018.09.157.

[18] Marvila, M. T., Azevedo, A. R. G. de, & Vieira, C. M. F. (2021). Reaction mechanisms of alkali-activated materials. Revista IBRACON de Estruturas e Materiais, 14(3). doi:10.1590/s1983-41952021000300009.

[19] Amigó, J. M., Serrano, F. J., Kojdecki, M. A., Bastida, J., Esteve, V., Reventós, M. M., & Martí, F. (2005). X-ray diffraction microstructure analysis of mullite, quartz and corundum in porcelain insulators. Journal of the European Ceramic Society, 25(9), 1479–1486. doi:10.1016/j.jeurceramsoc.2004.05.019.

[20] Liu, T., Zhang, J., Wu, J., Liu, J., Li, C., Ning, T., Luo, Z., Zhou, X., Yang, Q., & Lu, A. (2019). The utilization of electrical insulators waste and red mud for fabrication of partially vitrified ceramic materials with high porosity and high strength. Journal of Cleaner Production, 223, 790–800. doi:10.1016/j.jclepro.2019.03.162.

[21] Amari, S., Darestani, M., Millar, G. J., Rintoul, L., & Samali, B. (2019). Microchemistry and microstructure of sustainable mined zeolite-geopolymer. Journal of Cleaner Production, 234, 1165–1177. doi:10.1016/j.jclepro.2019.06.237.

[22] Iqbal, Y., & Lee, W. E. (2000). Microstructural evolution in triaxial porcelain. Journal of the American Ceramic Society, 83(12), 3121–3127. doi:10.1111/j.1151-2916.2000.tb01692.x.

[23] Zegardło, B., Szeląg, M., & Ogrodnik, P. (2016). Ultra-high strength concrete made with recycled aggregate from sanitary ceramic wastes – The method of production and the interfacial transition zone. Construction and Building Materials, 122, 736–742. doi:10.1016/j.conbuildmat.2016.06.112.

[24] Vitola, L., Pundiene, I., Pranckeviciene, J., & Bajare, D. (2020). The impact of the amount of water used in activation solution and the initial temperature of paste on the rheological behaviour and structural evolution of metakaolin-based geopolymer pastes. Sustainability (Switzerland), 12(19), 8216. doi:10.3390/su12198216.

[25] Chi, M. (2015). Effects of modulus ratio and dosage of alkali-activated solution on the properties and micro-structural characteristics of alkali-activated fly ash mortars. Construction and Building Materials, 99, 128–136. doi:10.1016/j.conbuildmat.2015.09.029.

[26] Geraldo, R. H., Fernandes, L. F. R., & Camarini, G. (2021). Mechanical properties of porcelain waste alkali-activated mortar. Open Ceramics, 8, 100184. doi:10.1016/j.oceram.2021.100184.

[27] Xu, N., Li, S., Li, Y., Xue, Z., Yuan, L., Zhang, J., & Wang, L. (2015). Preparation and properties of porous ceramic aggregates using electrical insulators waste. Ceramics International, 41(4), 5807–5811. doi:10.1016/j.ceramint.2015.01.009.

[28] ASTM C618-19. (2022). Standard Specification for Coal Fly Ash and Raw or Calcined Natural Pozzolan for Use in Concrete. ASTM International, Pennsylvania, United States. doi:10.1520/C0618-19.

[29] Li, H. Jian, & Sun, H. hu. (2009). Microstructure and cementitious properties of calcined clay-containing gangue. International Journal of Minerals, Metallurgy and Materials, 16(4), 482–486. doi:10.1016/S1674-4799(09)60084-4.

[30] Belmokhtar, N., El Ayadi, H., Ammari, M., & Ben Allal, L. (2018). Effect of structural and textural properties of a ceramic industrial sludge and kaolin on the hardened geopolymer properties. Applied Clay Science, 162, 1–9. doi:10.1016/j.clay.2018.05.029.

[31] ASTM C187-04. (2010) Standard Test Method for Normal Consistency of Hydraulic Cement. ASTM International, Pennsylvania, United States. doi:10.1520/C0187-04.

[32] ASTM C642-21. (2022). Standard Test Method for Density, Absorption, and Voids in Hardened Concrete. ASTM International, Pennsylvania, United States. doi:10.1520/C0642-21.

[33] Collins, F., & Sanjayan, J. G. (1999). Strength and shrinkage properties of alkali-activated slag concrete containing porous coarse aggregate. Cement and Concrete Research, 29(4), 607–610. doi:10.1016/S0008-8846(98)00203-8.

[34] Vieira, A. W., Innocentini, M. D. de M., Mendes, E., Gomes, T., Demarch, A., Montedo, O. R. K., & Angioletto, E. (2017). Comparison of Methods for Determining the Water Absorption of Glazed Porcelain Stoneware Ceramic Tiles. Materials Research, 20(suppl 2), 637–643. doi:10.1590/1980-5373-mr-2017-0089.

[35] Reddy, M. S., Dinakar, P., & Rao, B. H. (2016). A review of the influence of source material's oxide composition on the compressive strength of geopolymer concrete. Microporous and Mesoporous Materials, 234, 12–23. doi:10.1016/j.micromeso.2016.07.005.

[36] ASTM C191-8a. (2019). Standard Test Method for Time of Setting of Hydraulic Cement by Vicat Needle. ASTM International, Pennsylvania, United States. doi:10.1520/C0191-18A.

[37] Temuujin, J., Williams, R. P., & van Riessen, A. (2009). Effect of mechanical activation of fly ash on the properties of geopolymer cured at ambient temperature. Journal of Materials Processing Technology, 209(12–13), 5276–5280. doi:10.1016/j.jmatprotec.2009.03.016.

[38] Linda Bih, N., Aboubakar Mahamat, A., Hounkpè Bidossèssi, J., Azikiwe Onwualu, P., & Boakye, E. E. (2021). The effect of polymer waste addition on the compressive strength and water absorption of geopolymer ceramics. Applied Sciences (Switzerland), 11(8), 3540. doi:10.3390/app11083540.

[39] Malkawi, A. B., Nuruddin, M. F., Fauzi, A., Almattarneh, H., & Mohammed, B. S. (2016). Effects of Alkaline Solution on Properties of the HCFA Geopolymer Mortars. Procedia Engineering, 148, 710–717. doi:10.1016/j.proeng.2016.06.581.

[40] Jindal, B. B., Singhal, D., Sharma, S. K., Ashish, D. K., & Parveen, P. (2017). Improving compressive strength of low calcium fly ash geopolymer concrete with alccofine. Advances in Concrete Construction, 5(1), 17–29. doi:10.12989/acc.2017.5.1.17.

[41] Cristelo, N., Coelho, J., Miranda, T., Palomo, Á., & Fernández-Jiménez, A. (2019). Alkali activated composites – An innovative concept using iron and steel slag as both precursor and aggregate. Cement and Concrete Composites, 103, 11–21. doi:10.1016/j.cemconcomp.2019.04.024.

[42] Ukritnukun, S., Koshy, P., Rawal, A., Castel, A., & Sorrell, C. C. (2020). Predictive model of setting times and compressive strengths for low-alkali, ambient-cured, fly ash/slag-based geopolymers. Minerals, 10(10), 1–21. doi:10.3390/min10100920.

[43] Zulkifli, N. N. I., Abdullah, M. M. A. B., Przybył, A., Pietrusiewicz, P., Salleh, M. A. A. M., Aziz, I. H., Kwiatkowski, D., Gacek, M., Gucwa, M., & Chaiprapa, J. (2021). Influence of sintering temperature of kaolin, slag, and fly ash geopolymers on the microstructure, phase analysis, and electrical conductivity. Materials, 14(9), 2213. doi:10.3390/ma14092213.

[44] Liew, Y. M., Kamarudin, H., Al Bakri, A. M. M., Bnhussain, M., Luqman, M., Nizar, I. K., Ruzaidi, C. M., & Heah, C. Y. (2013). Effect of curing regimes on metakaolin geopolymer pastes produced from geopolymer powder. Advanced Materials Research, 626, 931–936. doi:10.4028/www.scientific.net/AMR.626.931.

[45] Sindhunata, Van Deventer, J. S. J., Lukey, G. C., & Xu, H. (2006). Effect of curing temperature and silicate concentration on fly-ash-based geopolymerization. Industrial and Engineering Chemistry Research, 45(10), 3559–3568. doi:10.1021/ie051251p.

[46] Gowram, I. (2022). Experimental and analytical study of high-strength concrete containing natural zeolite and additives. Civil Engineering Journal, 8(10), 2318-2335. doi:10.28991/CEJ-2022-08-10-019.

[47] Ranjbar, N., Kashefi, A., & Maheri, M. R. (2018). Hot-pressed geopolymer: Dual effects of heat and curing time. Cement and Concrete Composites, 86, 1–8. doi:10.1016/j.cemconcomp.2017.11.004.

[48] Mallikarjuna Rao, G., & Gunneswara Rao, T. D. (2015). Final Setting Time and Compressive Strength of Fly Ash and GGBS-Based Geopolymer Paste and Mortar. Arabian Journal for Science and Engineering, 40(11), 3067–3074. doi:10.1007/s13369-015-1757-z.

[49] Vikas, G., & Rao, T. D. G. (2021). Setting Time, Workability and Strength Properties of Alkali Activated Fly Ash and Slag Based Geopolymer Concrete Activated with High Silica Modulus Water Glass. Iranian Journal of Science and Technology - Transactions of Civil Engineering, 45(3), 1483–1492. doi:10.1007/s40996-021-00598-8.

[50] Ababneh, A., Matalkah, F., & Aqel, R. (2020). Synthesis of kaolin-based alkali-activated cement: carbon footprint, cost and energy assessment. Journal of Materials Research and Technology, 9(4), 8367–8378. doi:10.1016/j.jmrt.2020.05.116.

[51] Karakoç, M. B., Türkmen, İ., Maraş, M. M., Kantarci, F., Demirboğa, R., & Uğur Toprak, M. (2014). Mechanical properties and setting time of ferrochrome slag based geopolymer paste and mortar. Construction and Building Materials, 72, 283–292. doi:10.1016/j.conbuildmat.2014.09.021.

[52] Ranjbar, N., Kuenzel, C., Spangenberg, J., & Mehrali, M. (2020). Hardening evolution of geopolymers from setting to equilibrium: A review. Cement and Concrete Composites, 114, 103729. doi:10.1016/j.cemconcomp.2020.103729.

[53] Elyamany, H. E., Abd Elmoaty, A. E. M., & Elshaboury, A. M. (2018). Setting time and 7-day strength of geopolymer mortar with various binders. Construction and Building Materials, 187, 974–983. doi:10.1016/j.conbuildmat.2018.08.025.

[54] Nagajothi, S., Elavenil, S., Angalaeswari, S., Natrayan, L., & Mammo, W. D. (2022). Durability studies on fly ash based geopolymer concrete incorporated with slag and alkali solutions. Advances in Civil Engineering, 2022. doi:10.1155/2022/7196446.

[55] Olivia, M., & Nikraz, H. (2011). Strength and water penetrability of fly ash geopolymer concrete. Journal of Engineering and Applied Sciences, 6(7), 70-78.

[56] Lavanya, G., & Jegan, J. (2015). Durability Study on High Calcium Fly Ash Based Geopolymer Concrete. Advances in Materials Science and Engineering, 2015, 1–7. doi:10.1155/2015/731056.

[57] Zaidi, F.H.A., Ahmad, R., Mustafa Al Bakri Abdullah, M., Faheem Mohd Tahir, M., Yahya, Z., Mastura Wan Ibrahim, W., & Syauqi Sauffi, A. (2019). Performance of Geopolymer Concrete when Exposed to Marine Environment. IOP Conference Series: Materials Science and Engineering, 551(1), 012092. doi:10.1088/1757-899x/551/1/012092.

[58] Zuaiter, M., El-Hassan, H., El-Maaddawy, T., & El-Ariss, B. (2022). Properties of Slag-Fly Ash Blended Geopolymer Concrete Reinforced with Hybrid Glass Fibers. Buildings, 12(8), 1114. doi:10.3390/buildings12081114.

[59] El-Hassan, H., & Elkholy, S. (2021). Enhancing the performance of Alkali-Activated Slag-Fly ash blended concrete through hybrid steel fiber reinforcement. Construction and Building Materials, 311, 125313. doi:10.1016/j.conbuildmat.2021.125313.

[60] Ramli, M. I. I., Salleh, M. A. A. M., Abdullah, M. M. A. B., Aziz, I. H., Ying, T. C., Shahedan, N. F., Kockelmann, W., Fedrigo, A., Sandu, A. V., Vizureanu, P., Chaiprapa, J., & Nergis, D. D. B. (2022). The Influence of Sintering Temperature on the Pore Structure of an Alkali-Activated Kaolin-Based Geopolymer Ceramic. Materials, 15(7). doi:10.3390/ma15072667.

[61] Arslan, A. A., Uysal, M., Yılmaz, A., Al-mashhadani, M. M., Canpolat, O., Şahin, F., & Aygörmez, Y. (2019). Influence of wetting-drying curing system on the performance of fiber reinforced metakaolin-based geopolymer composites. Construction and Building Materials, 225, 909-926. doi:10.1016/j.conbuildmat.2019.07.235.

[62] Manjunath, G. S., Giridhar, C., & Jadhav, M. (2011). Compressive Strength Development in Ambient Cured Geo-polymer Mortar. International Journal of Earth Sciences and Engineering, 4(6), 830-834.

[63] Zhang, P., Wang, K., Wang, J., Guo, J., & Ling, Y. (2021). Macroscopic and microscopic analyses on mechanical performance of metakaolin/fly ash based geopolymer mortar. Journal of Cleaner Production, 294, 126193. doi:10.1016/j.jclepro.2021.126193.

[64] Cheng, T. W., & Chiu, J. P. (2003). Fire-resistant geopolymer produce by granulated blast furnace slag. Minerals Engineering, 16(3), 205–210. doi:10.1016/S0892-6875(03)00008-6.

[65] Wang, J. W., & Cheng, T. W. (2003). Production geopolymer materials by coal fly ash. Proceedings of the 7th International Symposium on East Asian Resources Recycling Technology, 10-14 November, 2003, Tainan, Taiwan.

[66] Mohd Mortar, N. A., Abdullah, M. M. A. B., Abdul Razak, R., Abd Rahim, S. Z., Aziz, I. H., Nabiałek, M., Jaya, R. P., Semenescu, A., Mohamed, R., & Ghazali, M. F. (2022). Geopolymer Ceramic Application: A Review on Mix Design, Properties and Reinforcement Enhancement. Materials, 15(21), 7567. doi:10.3390/ma15217567.

[67] Poornima, N., Katyal, D., Revathi, T., Sivasakthi, M., & Jeyalakshmi, R. (2021). Effect of curing on mechanical strength and microstructure of fly ash blend GGBS geopolymer, Portland cement mortar and its behavior at elevated temperature. Materials Today: Proceedings, 47, 863–870. doi:10.1016/j.matpr.2021.04.087.

[68] Girish, M. G., Shetty, K. K., & Nayak, G. (2022). Synthesis of Fly-ash and Slag Based Geopolymer Concrete for Rigid Pavement. Materials Today: Proceedings, 60, 46–54. doi:10.1016/j.matpr.2021.11.332.

[69] Ma, X., Zhao, Y., Liu, M., Xia, Y., & Yang, Y. (2023). Sodium gluconate as a retarder modified sewage sludge ash-based geopolymers: Mechanism and environmental assessment. Journal of Cleaner Production, 138317. doi:10.1016/j.jclepro.2023.138317.

[70] Hájková, P. (2018). Kaolinite claystone-based geopolymer materials: Effect of chemical composition and curing conditions. Minerals, 8(10), 444. doi:10.3390/min8100444.

[71] Matalkah, F., Aqel, R., & Ababneh, A. (2020). Enhancement of the Mechanical Properties of Kaolin Geopolymer Using Sodium Hydroxide and Calcium Oxide. Procedia Manufacturing, 44, 164–171. doi:10.1016/j.promfg.2020.02.218.